# Parkfield revisited: I. Data retrieval

**Cinna Lomnitz[1] and Chao-jun Zhang[2]**
[1]UNIVERSIDAD NACIONAL AUTONOMA DE MEXICO, INSTITUTO DE GEOFISICA, CIUDAD UNIVERSITARIA, D.F. 04510, MEXICO
[2]CHINA EARTHQUAKE NETWORK CENTER, BEIJING 100045, CHINA

## ABSTRACT

The Parkfield earthquake prediction experiment (1985–2004) was designed to monitor stress accumulation in the lithosphere related to an impending earthquake on the San Andreas fault. However, no precursory signals were detected prior to the 2004 Parkfield earthquake (M6.0). In this paper we re-examine the long-term borehole strain records at Parkfield (Langbein et al., 2006). We find that they are consistent with a stationary tectonic stress field on the order of 55 MPa in the direction of the fault. This is the first measurement of far-field tectonic stresses from borehole strainmeter records. It suggests that logarithmic creep strains from boreholes can be used to interpret the state of stress in the lithosphere surrounding the San Andreas fault.

Symmetry of the experimental setup suggests conformal mapping is a useful transformation to interpret the state of stress around a cavity in a prestressed halfspace. The borehole inverts the sign of the displacement, so that compressional tectonic stresses generate extensional strains at the borehole boundary. The stress energy field is conserved under conformal transformation (Noether's theorem). This transformation facilitates recovery of the state of stress in the lithosphere from long-term Parkfield strain records. Ergodicity constrains the form of the creep function in long-term experiments as follows: $\varepsilon(t) = \frac{1}{M}\left[\sigma(t) + \int_0^\infty \sigma(\tau)\varphi(t-\tau)d\tau\right]$, where the decay function is $\varphi(t) = \frac{q\omega_0}{1+\omega_0 t}$.

In conclusion, available experimental evidence suggests that the Parkfield borehole strainmeter data preceding the 2004 earthquake are consistent with a tectonic stress estimate on the order of 55 MPa in agreement with the tectonics of the area. No evidence of long-term stress accumulation has been found.

LITHOSPHERE; v. 1; no. 4; p. 227–234. doi: 10.1130/L14.1

## AFTERMATH OF AN EXPERIMENT

This is the first of a series of articles on the Parkfield experiment (1985–2004). In the present paper we discuss an important data source. Long-term strain records from a tight network of three GTSM tensor borehole strainmeter stations at Parkfield, as available on the internet site of the manufacturer (http://www.gtsmtechnologies.com/NEHRP/images/plots/rsjt1.jpg *through* rgat4.jpg), contain large time-decaying strain effects previously attributed to a combination of "borehole relaxation" and "grout expansion." Because the data might be unrelated to the resident tectonic stresses in the lithosphere, they were discarded or used with caution. Short-term signals from the same stations were successfully used despite some remaining issues of calibration.

An effort to explore the feasibility of a reinterpretation of the Parkfield tensor strain observations is timely and justified by the importance of the data. Gwyther (1995) concluded that measurements of tectonic strain have "historically been undervalued in earthquake studies." There is no comparable set of tectonic strain observations spanning a period of 20 years before a major earthquake, and the analysis of the data yields previously unsuspected instrumental issues.

Retrieval of the long-term data, even at the microstrain level, turns out to be an absorbing and complex task. There is more material than could be handled in a single paper. In future papers, we hope to discuss important issues, including the suggestion of alternative models of earthquake generation, which can only be mentioned in passing here.

We propose that the tectonic stress field at Parkfield may be estimated from available long-term strain records. The tensor strainmeter stations straddle the San Andreas fault, and the tectonic stress field appears to be time-invariant for a substantial part of the 1966–2004 interseismic period, including the years 1985–2004 monitored by the Parkfield experiment. The decay curves observed over this experimental time span are consistent with the interpretation of creep response of the rock to strain release at the time of deployment of the borehole instruments between 8 November and 7 December 1986.

Three-component strain data at Parkfield borehole stations are shown in Figures 1–3. All three stations are within 5 km of the San Andreas fault and within 15 km of the epicenter of the 2004 earthquake. Time is computed from the date of deployment. Extension is *up,* and orientations of the strain components are shown in Table 1 in degrees east of north. The initial curves to the left of the zero crossings are attributed to strain transients caused by expansive grout. These semilog plots show that the creep response fits logarithmic decay in time, and that the fit improves with time. At long times the raw data fits the theoretical logarithmic creep curves so closely that the two curves overlap. This finding represents the essential point of this paper.

## DATA RETRIEVAL

Figure 1 shows the long-term strain output at station DonnaLee (DLT), at Parkfield. This station is on the North America plate, 5 km east of the trace of the San Andreas fault at a depth of 174 m. Similar records are available for stations Froelich and Eades (Figs. 2 and 3). Froelich (FLT) is on the Pacific plate, ~1 km west of the fault at a depth of 237 m, and Eades (EDT) is on the North America plate, ~1 km east of the San Andreas fault trace at 271 m depth. EDT station failed in 2002 due to cable leakage: sensor EDT3 apparently died down gradually (Fig. 2). Station EDT was only used for helping establish the stress-strain-time relations. The signal at station DLT was contaminated by seasonal fluctuations in an aquifer, but the amplitude of the

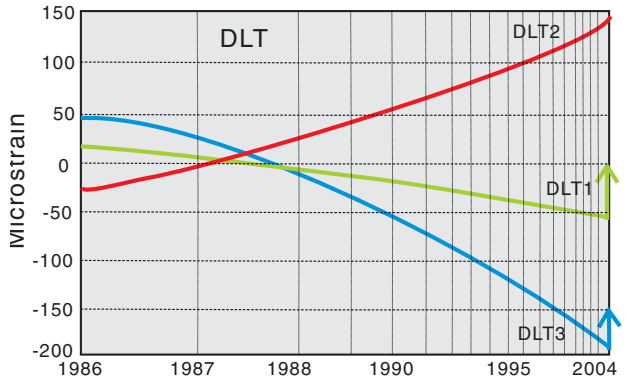


**Figure 1. Three-component, smoothened mean daily strains at Parkfield station DonnaLee (DLT; depth 174 m). Extension is up and orientations of the strain components are found in Table 2. The fit of the raw data to a logarithmic creep function improves with time.**

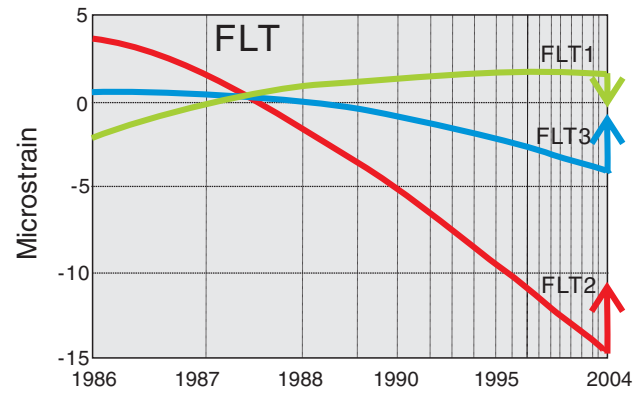


**Figure 2. As in Figure 1, for station Froelich (FLT; depth 237 m).**

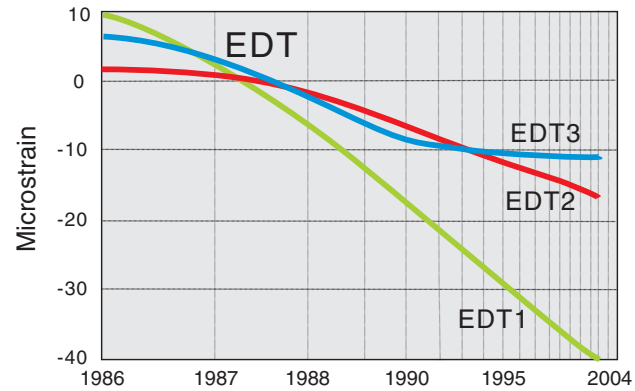


**Figure 3. As in Figure 1, for station Eades (EDT; depth 271 m). A cable was damaged at the time of inserting the instrument into the borehole, causing the malfunction in EDT3. The station was closed in 2002. Orientations (north of east) of the strain components are as follows: EDT1, 84.25°; EDT2, –35.75°; EDT3, 24.25°.**

TABLE 1. GTSM TECHNOLOGIES TENSOR STRAINMETER STATIONS

| Name of station | Abbreviation | Depth (m) | Date of deployment | Geologic setting |
|---|---|---|---|---|
| DonnaLee | DLT | 174 | 8 November 1986 | Franciscan sandstone |
| Eades | EDT | 271 | 13 November 1986 | Franciscan sandstone |
| Froelich | FLT | 237 | 7 December 1986 | Salinian granite |

noise was less than one microstrain. For other relevant issues, including San Andreas tectonics, fault geometry or fault healing, see the *Bulletin of the Seismological Society of America* (2006) Special Issue, Part B.

The Parkfield experiment was disappointing to some and a source of insight to others. An earthquake had been predicted to occur before 1994, but the prediction window lapsed and no earthquake occurred. Eleven years later, on 28 September 2004, an earthquake of the predicted magnitude (Mw 6.0) did occur at the predicted location (Murray and Langbein, 2006). This event was not preceded by precursory effects. The absence of precursors is one of the challenges posed by the Parkfield experiment (Johnston et al., 2006; Harris and Arrowsmith, 2006).

A shift in the strategy of U.S. earthquake research occurred after the 2004 Parkfield earthquake. The Plate Boundary Observatory (PBO), one of three components of a new approach to earthquake research, is part of the Earthscope project funded by the National Science Foundation, along with USArray and San Andreas Fault Observatory at Depth (SAFOD). PBO is designed to explore the structure and evolution of the North American continent and the processes related to earthquakes and volcanoes. It is installing an array of high-precision global positioning system (GPS) monuments, borehole strainmeters, and tiltmeters throughout the western United States. UNAVCO, a membership-governed consortium funded by the National Science Foundation and National Aeronautics and Space Administration (NASA), manages PBO. Upon completion, there will be 875 GPS stations, 103 borehole strainmeters, and five laser strainmeters throughout the western United States and Alaska.

The global positioning system (GPS), as originally developed by the United States Department of Defense, is the backbone of PBO. This geodetic surveying system uses between 24 and 32 medium Earth orbit satellites that transmit microwave signals, which enable GPS receivers to determine location, time, and relative velocities at any station on Earth. The transform cluster of GPS stations around the San Andreas fault can detect sub-cm motion at a 15-s sampling rate and generates one data file every 24 h. "How does accumulated strain lead to earthquakes?" is a question being explicitly addressed by the EarthScope project and the PBO. It was basically the same question posed by the Parkfield experiment.

A GTSM tensor strain module is a sensitive sensor housed in a 12.5-cm-diameter, airtight, cylindrical, horizontal stainless-steel box. A variable-capacitance transducer is welded to opposite walls of the module; it measures relative displacements between the walls of the box. The mean gap between capacitor plates is ~0.2 mm. The plates are mechanical cantilevers, so that each plate has a spring constant, an effective mass, and a resonant frequency that is proportional to the thickness and inversely proportional to the square of the length of the plate (Cleland, 2003).

A strainmeter assembly consists of three strain module units stacked on top of each other at 120° angles to measure three horizontal components of the strain tensor. A vertical component is not provided. In the field, the strainmeter is inserted in a 6-in. borehole drilled down to a depth of ~200 m, with a ½-in. clearance between the strainmeter and the hole. The bottom four meters of the hole are reamed and filled with expansive grout; then the strainmeter is lowered into the mushy grout and left to cure.

Factory calibration includes verifying the wall thickness response, the interelectrode gap settings, and the circuit electronics. The units are factory tested under hydrostatic loads. Final calibration at the nanostrain level is done in situ, with the instrument grouted into the bottom of the hole. Tidal strains are measured and compared with theoretical earth strains. These tidal signals turn out to be smaller than 1 μstrain and much smaller than the creep response of the rock to unloading, or the strain response to grout expansion. Iterative comparisons of the observed tidal signal with theoretical amplitudes and phases of the two main tides O1 and M2 may involve significant errors, which can be estimated when independent tidal

observations happen to be available (Gladwin and Hart, 1985; Hart et al., 1996; Roeloffs et al., 2004; Roeloffs, 2005).

GTSM instruments are not reset to zero strain. The reference strain is roughly pegged to the local mean tidal level. This should be adequate for our present purpose because we are interested in relative strains at the microstrain level only.

## NOETHER'S THEOREM

We propose to use conformal mapping as an exploratory approach to understand a phenomenon loosely described as "borehole relaxation" and "grout curing" (Roeloffs, 2005). It concerns the initial behavior of the strainmeter after insertion. A transformation that preserves local angles is useful in cavity problems where the geometry can be changed into a more convenient configuration to handle (Bath and Berkhout, 1984; Claerbout and Dellinger, 1987). Thus a cavity of any shape may be mapped into a halfspace, and the halfspace may be mapped into the cavity.

First we show that the stress configuration remains invariant under transformation. Consider a borehole in a halfspace (Fig. 4) and suppose a particle is moving on a radial line with Lagrangian $L(q, \dot{q})$, where $q$ is its position and $\dot{q} = dq/dt$ is its velocity (Baez, 2002). The momentum of the particle is defined as:

$$p = dL / d\dot{q} \tag{1}$$

and the force on it is:

$$F = dL / dq. \tag{2}$$

The rate of change of momentum is equal to the force

$$\dot{p} = F. \tag{3}$$

Now, if the Lagrangian $L$ has a symmetry under a one-parameter transformation $q \rightarrow q(s)$ as in the case of conformal mapping, the stress energy is a conserved quantity, i.e., $\dot{C} = 0$, where $C = pdq(s)/ds$ (Marinho, 2007).

Consider the symmetry of our experimental setup. Let a horizontal section across the borehole be called the $z$-plane (Fig. 4). Domain $D$ (*left*) may be mapped into domain $D'$ (*right*) by using the mapping transformation $w = 1/z$, where $w$ is the plane of the transformed domain, the radius of the borehole is taken as unity and the axis of the borehole as the origin of the inversion. Thus the borehole is conveniently transformed into a solid cylinder of rock of the same dimensions and vice versa. This symmetry entails conservation of the stress field, because any differentiable symmetry of the action of a physical system has a corresponding conservation law (Noether's theorem; see Baez, 2002).

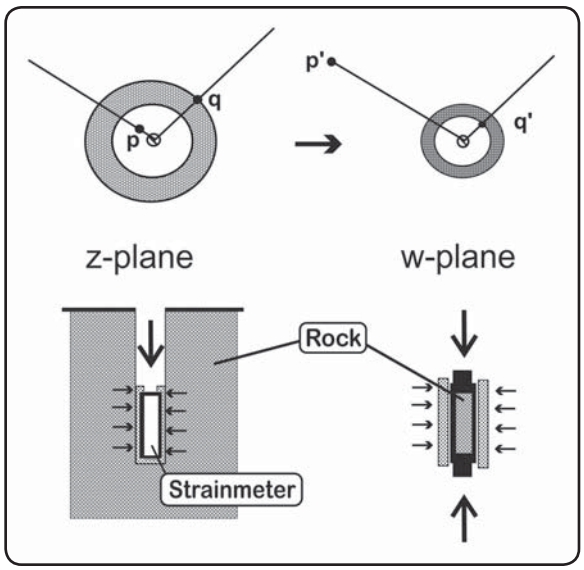


**Figure 4. Conformal mapping from configuration *D* (left) into *D′* (right). Points *p* and *q* are mapped into points *p′* and *q′*.**

Consider now the following:

*Proposition 1*. Strains generated by any stress field around a cavity are equal and opposite in sign to those produced in an equivalent conformal triaxial test.

*Sketch of Proof.* Conformal mapping transforms the original borehole configuration into a symmetrical configuration. But equivalently, a cavity may be treated as a negative anomaly, or a body of negative density and elastic parameters in the halfspace. After a conformal transformation, the boundaries of the cavity in the $z$-plane are identical with the boundaries of a rock specimen in the $w$-plane. Any external points such as $q$ (Fig. 4) will be mapped inside the cavity, and any inner ones such as $p$ outside it. Thus any extensional strains in the $z$-plane will be mapped as compressional strains in the $w$-plane, and vice versa. But the stress field is conserved: therefore the strains in either case will be the same. In conclusion, a specimen of rock in a symmetrical triaxial test will be deformed in the opposite way as would a cavity under the same set of external loads.

Thus a circular cavity will be elongated, not flattened, in the direction of maximum compressional resident stresses (Fig. 5). This may seem counterintuitive, but the result has been analytically confirmed (Kirsch, 1898; Lund, 2000). If the principal compressive stress acts in the $x$-direction, the cavity is elongated in the same direction. Because the rock will creep under stresses that were present in the prestressed halfspace before insertion of the cavity, we may calculate the tectonic stress field from the observed deformations, provided that the change in sign is taken into account. The result may be extended to the case of a cavity filled with a low-impedance material, such as mortar or grout.

## ERGODICITY

Let us now derive the mathematical form of the stress-strain equation. Experiments with iron springs in tension enabled Robert Hooke to declare that extension was always proportional to force (ut tensio sic vis). The time variable $t$ was kept implicit, because the mathematical apparatus for representing his results by a time-dependent linear constitutive equation was not available at the time. Such an equation was developed by Vito Volterra and is named after him:

$$\varepsilon(t) = \frac{1}{M}\left[\sigma(t) + \int_0^{\infty} \sigma(\tau)\varphi(t-\tau)d\tau\right]. \tag{4}$$

Here $\sigma$ is stress, $\varepsilon$ is strain, $M$ is the elastic modulus, and $\varphi(t)$ is a decay function that is positive, as required by causality. According to the superposition principle for linear systems, the space-time response caused by successive stress inputs equals the sum of the corresponding individual responses, as predicted by Equation 4. This behavior agrees with observations in rocks at moderate loads and temperatures. Igneous rocks behave much as other polycrystalline materials, and the upper lithosphere is relatively cool: thus the Hooke-Volterra law is relevant to rock mechanics (Lomnitz, 1956, 1957). The two terms inside square brackets represent *elastic* and *anelastic* behavior.

The anelastic part of Equation 4 is known as *linear creep.* The form of the decay function $\varphi(t)$ is of particular interest because it governs the long-

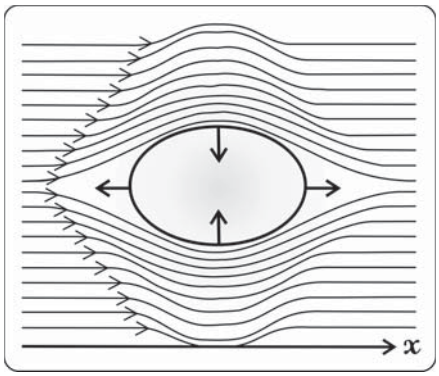


**Figure 5. A borehole in a homogeneous horizontal compressional stress field (after Lund, 2000). Strains at the cavity boundary (heavy arrows) are reversed so that extension of the borehole occurs in the direction of maximum compressional stress.**

term behavior of the material. When a stress-strain experiment is conducted over a period of time longer than one year, it may be assumed that all accessible microstates in state space are equally probable. Introducing an ergodic hypothesis, the time average of process parameter $M$ (the elastic modulus) will tend to equal the space average of the same parameter:

$$\lim_{t\to\infty}\frac{d\varepsilon(t)}{d\sigma(t)}=\frac{d\varepsilon(x,y,z)}{d\sigma(x,y,z)}=\frac{1}{M} \tag{5}$$

at almost all points in phase space and for sufficiently long time intervals (Arnold and Avez, 1968).

Introducing the ergodic hypothesis into Equation 4, we find $d\varphi/dt = -\varphi(t)$, or

$$\varphi(t)=\frac{q\omega_0}{1+\omega_0 t}, \tag{6}$$

also known as Omori's law of aftershock frequency (Enescu et al., 2009). The parameters $q$ and $\omega_0$ are material constants; the frequency $\omega_0$ may attain values of several thousand Hz, while the dimensionless creep modulus $q$ is on the order of magnitude of $1/Q$.

For the special case of a constant load $\sigma_0$ applied at time $t = 0$, we may write

$$\varepsilon(t)=\frac{\sigma_0}{M}\left[1+q\log(1+\omega_0 t)\right], \tag{7}$$

known as the equation of *logarithmic creep.* Notice that the strain $\varepsilon(t)$ increases approximately as the logarithm of time when $\omega_0 \gg 1$, as observed in Figure 1.

Logarithmic strain-time curves have been observed experimentally in rocks for many years (e.g., Griggs and Handin, 1960; Jeffreys, 1970; see also Figs. 1–3). In the cool upper lithosphere, this behavior is often described as *transient* creep. It is the constitutive equation derived from ergodicity. In rheology, it corresponds to a generalized Maxwell model.

The strain data fit Equation 7 quite well. Hart et al. (1996) assumed that the long-term strain signals should also contain a linear term $ct$ corresponding to strain accumulation prior to the 2004 earthquake. Let us contrast Equation 7 against the alternative equation

$$\varepsilon(t)=\frac{\sigma_0}{M}\left[1+q\log(1+\omega_0 t)\right]+ct, \tag{8}$$

where $q$ and $c$ must have the same sign, if the accumulated strain is to be released in a subsequent earthquake. Changing to semilog coordinates ($x = \log t$) as in Figures 1–3, we have approximately, for large values of $t$,

$$\varepsilon(x)\approx\frac{\sigma_0}{M}[const+qx]+ce^x. \tag{9}$$

The exponential term $ce^x$ must dominate the linear term in $x$ for positive increasing values of $x$. But the opposite is observed: in Figures 1–3, the strain curve $\varepsilon(x)$ tends to straighten out and become more rectilinear with time. This is a sensitive test: for hypothetical strain accumulation rates as low as $c = 1$ μstrain per year, the curvature of $\varepsilon(x)$ should increase significantly by the time the 2004 earthquake is approached. A logarithmic fit is superior to other functional adjustment methods that have been proposed, because it requires no periodic updating and uses fewer free parameters than does, e.g., the fit with two exponential functions.

In conclusion, the term in $e^x$, if it exists, is amply overshadowed by the creep effect. Creep strain amplitudes of 10–200 microstrains were recorded during an 18-year period (see Figs. 1–3), as compared to a near-field coseismic strain offset of less than 5 microstrains in the 2004 earthquake (Johnston et al., 2006).

## AN INTERPRETATION OF PARKFIELD BOREHOLE OBSERVATIONS

We observe that (1) the borehole shows extension in the direction of the tectonic stress field, (2) the grout tends to expand in the same direction, and (3) the strainmeter module deforms into an ellipse with its major axis extended normally to the direction of the tectonic stress field. These observations may be confirmed by inspection of the long-term strain records.

These features may be explained as follows. Consider a transverse section of the borehole (Fig. 6), where the strainmeter occupies the dark-shaded central area. The clearance between the strainmeter and the walls of the borehole is filled with expansive grout meant to exert a uniform pressure on the strainmeter and to ensure perfect coupling to the borehole walls. Actually, however, the strainmeter deforms into an ellipse, because the strains are extensional in some directions and contractional in others. This asymmetry may be observed, e.g., in Figure 1. It cannot be attributed to the grout, or to the borehole: both are symmetrical. It must be due to the resident tectonic stresses in the lithosphere. Thus the long-term strains at Parkfield do reflect the state of stress in the lithosphere.

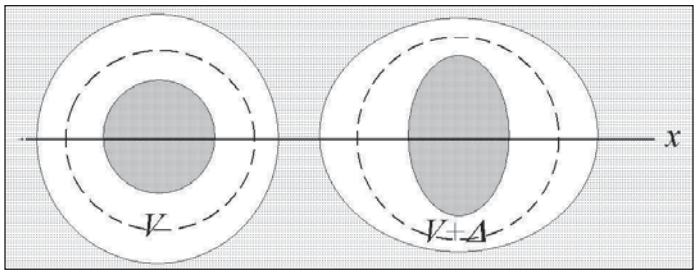


**Figure 6. Deformation of a donut-shaped ring of grout of volume $V$ when expanded to $V + \Delta$ inside an elliptical borehole section. The dotted circle is the equator of the ring of grout.**

Consider the following:

*Proposition 2.* When the donut-shaped clearance between the strainmeter and the cavity wall is occupied by expanding grout, the strainmeter module deforms into an ellipse with its major axis normal to the direction $x$ of principal compression of the ambient stress field.

*Sketch of Proof.* The borehole elongates in the $x$-direction (Proposition 1). Suppose the perimeter of the borehole remains constant. Let $a$ and $b$ be the semi-major and semi-minor axes of the borehole (Fig. 6). Because the borehole is under compression, its total volume tends to decrease during deformation while the volume $V$ of the grout expands to $V + \Delta$. This must occur largely at the expense of the central dark-shaded strainmeter.

Let ellipticity be defined as $E = (a - b)/a$. Then the total area of the section is $A = \pi a^2(1 - E)$. The case $E < 0$ is irrelevant because it represents a permutation of the axes, so that $a \leftrightarrow b$, which is equivalent to rotating the reference frame by 90°. Thus it is sufficient to consider the case $E \geq 0$. The area $A$ is maximized when $1 - E = 1$, or $E = 0$. In other words, the ellipse of maximum area is the circle of radius $r = a$. But the perimeter of this circle is $P = 2\pi r$. Suppose that $a \neq r$: then the perimeter of the ellipse is $P' \neq 2\pi r$. But the perimeter of the ellipse is held constant: therefore we must have $P' = P$. It follows that the ellipse of maximum area is such that $a = r$.

Conversely, the ellipse of minimum perimeter at constant area $A$ is the circle $a = r$. Consider the ratio $A/P$ between the area and the perimeter of the ellipse. If the area is maximized for $a = b$ and $P$ invariant, it must also be true that $P$ is minimized for $a = b$ and $A$ invariant, because $\partial A/\partial P$ is the reciprocal of $\partial P/\partial A$. Proposition 2 thus predicts that under pressure from expanding grout, the strainmeter module is constrained to deform into an ellipse, since any ellipse has a smaller area than has the corresponding circle of the same perimeter $P$.

We have shown that a circle of constant perimeter must deform into an ellipse when its area is reduced. But why should the outer and inner semi-major axes be orthogonal to each other? This is indeed the experimental finding at Parkfield (cf. Fig. 1). On Figure 6, the dashed line is the *equatorial circle*, a circle which remains invariant under deformation of the donut-shaped ring of grout. This deformation takes place under homogeneous expansion of the grout, so that the forces on both interfaces must balance independently of the value of the lithostatic pressure in the half-space. The pressure inside the donut is the same everywhere, so the angle of the interfaces with the normal must be conserved during deformation. This condition is satisfied if and only if one interface is the conformal transform of the other.

In conformal transformation, let the dashed equatorial circle be taken as reference and its radius as unity. Initially both the outer and the inner surface of the donut are circles. Let now the outer circle be elongated into an ellipse in the $x$ direction, as in Figure 6: the conformal map of this outer ellipse is an inner ellipse which is elongated in the $y$ direction, since all contractions are mapped into extensions and vice versa. This simple demonstration is valid for concentric circles of whatever radius inside the grout as well: this proves that an equatorial circle must exist, since there is a smooth transition while the two elliptical interfaces deform in opposite directions. This concludes our explanation of the initial behavior of the strain gauges when subjected to expanding grout.

What happens after the expansive energy of the grout has been spent? The strain record shows that all three components of deformation reverse direction at some early time we cannot observe, because the instrument has not yet settled down to its normal operating condition. Roughly speaking, the positive area below the strain curve represents the work done by the grout (Fig. 7, shaded area). After the time of maximum expansion has been reached, the strain rate changes sign and all three components recross the line of zero strain. This happens roughly 1.5 years (400–600 days) after deployment. From that time on, the sign of the strain rate is consistent with the deformation of the borehole.

Let us summarize Figure 7. At deployment the borehole is drilled, the strainmeter is inserted in the fluid grout, and the grout sets and starts expanding. Simultaneously, the rock is subjected to the resident tectonic stress in the lithosphere because of Newton's third law: for every action (drilling a hole and producing a cavity, thus removing the force that acted on the interface) there is an equal and opposite reaction (a tectonic force that equals and opposes the force that was removed). The reaction comes in two parts, according to Equation 7—an elastic part and a creep part. The elastic part of the strain is lost: it is not recorded because the strainmeter is not yet installed when the borehole is drilled. Now the grout sets and expands rapidly but its chemical energy is quickly spent. Days after deployment, the rate of expansion levels off and reverses on all strain components, because creep deformation and grout expansion act in opposite directions. The expansion of the grout initially countered the contraction caused by the resident tectonic stress; but some 18 months later the strain recrosses the zero-strain line. This means that the initial strain conditions are reestablished. But not quite: the rock has been deformed. It remembers the initial expansion, and this distorts the logarithmic strain response.

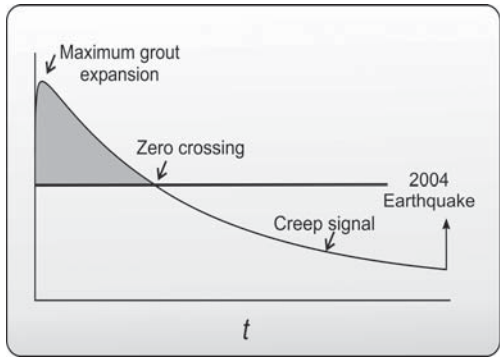


**Figure 7. A sketch of the creep response in the lithosphere after deployment of the strainmeter in the borehole and emplacement of expansive grout. Shaded area—effect of grout setting.**

Subsequent deformation consists largely of logarithmic creep because the grout has become an inert material. The tectonic stress acts on the strainmeter through this layer of solid grout. But now the tectonic stresses increasingly overpower the stresses from the expanding grout. Therefore the logarithmic fit to the creep curve improves over time.

Why did all nine Parkfield strain components recross the zero stress line nearly at the same time, namely ~18 months after deployment? This appears to be an instrumental constant. A similar delay may be observed at other GTSM stations where the same insertion procedure has been followed. It is the amount of time needed for a borehole of a standard diameter to recover from an episode of expansion caused by a standard type of grout. The role of the grout in deployment is somewhat unclear: the overall performance of borehole strainmeters could probably be improved by filling the hole with ordinary cement.

As expected, the direction of the coseismic stress drop in the 2004 earthquake was the opposite of the direction of the tectonic driving forces (Fig. 7, arrow). In terms of our strain records, the stress drop points in the opposite direction of the creep deformation (Figs. 1 and 2, arrows). But notice the important difference in strain amplitudes at DLT and FLT: this may be attributed to the substantial difference in rock types at each station. The strainmeter network straddles the San Andreas fault, a transcurrent plate boundary which places two totally different geologic sections in contact. Estimation of tectonic stress will depend crucially on our experimental knowledge of the viscoelastic parameters at each station. Because no cores were recovered from the boreholes, we depend on approximate values from the literature.

## THE TECTONIC STRESS FIELD IN THE LITHOSPHERE

A straightforward interpretation of Equation 7 suggests that the tectonic load $\sigma_0$ remained stationary during most of the interseismic period. This seems to be the implication of the straight-line fit of semilog graphs improving with time. No stress accumulation is noticed. No precursors

were detected. Johnston et al. (2006) confirmed that no coherent strain or pore pressure signal was observed in the near field during the weeks to seconds before the 2004 earthquake.

This result seems to contradict the hypothesis of stress accumulation preceding earthquakes. But stress accumulation is not necessarily a prerequisite for the occurrence of earthquakes. It is not required by the theory of elastic rebound. If we assume the Coulomb criterion as a failure condition, we may write:

$$\tau = \sigma_n \tan\phi + c, \tag{10}$$

where $\tau$ is the shear strength, $\sigma_n$ is the normal stress on the fault, $c$ is the cohesion, and $\phi$ is the angle of internal friction. The failure condition is $\tau = \sigma_s$, where $\sigma_s$ is the shear stress on the fault. This failure condition may be reached by two equivalent paths, namely (*a*) by accumulation of shear stress $\sigma_s$ until it overcomes the constant shear strength $\tau$, or (*b*) by degradation of shear strength $\tau$ until it is overcome by a constant shear stress $\sigma_s$. Other paths may be represented as combinations of these two paths.

Rocks in the laboratory will fail either way. Strength degradation takes place under steady-state loading conditions, i.e., in the absence of stress accumulation. Water or steam causes localized corrosion on preexisting cracks in the rock sample. Water, the main agent of strength degradation, corrodes silicates by replacing Si-O bonds with hydroxyl bonds –SiOH:HOSi– (NIRE, 1998). "Healing" (or strength recovery after an earthquake) is an active subject of research (see, e.g., Potyondy, 2007; Jeong et al., 2007; Singh and Verma, 2005; Szczepanik et al., 2003; Lockner, 1995; Blanpied et al., 1998; Li et al., 2006). Thus observations at Parkfield may fit either strength decay or stress accumulation or both, and neither is incompatible with the prevailing theory of elastic rebound.

Let us now proceed to calculate the resident stress field in the lithosphere. The results are tentative, because Parkfield rock cores are unavailable and the calibration of strainmeters seems uncertain, not least because of the large differences in stress-strain behavior from one rock type to another. DonnaLee (DLT) is in Franciscan basement rock, mainly sandstone, while Froelich (FLT) is in Salinian granitic rocks (see Table 1). Data from Eades (EDT) are irrelevant because the station failed and was not used. But we need the values of material constants to be inserted in Equation 7.

Table 2 lists the long-term strain amplitudes as recorded at stations DonnaLee and Froelich up to the 2004 earthquake. The principal strains in the lithosphere may be calculated from these data, as shown in Table 3. Angles are measured in degrees counterclockwise from the *x*-axis (north of east).

TABLE 2. CUMULATIVE 16.5-YEAR CREEP STRAINS AT PARKFIELD (1988–2004)

| Station | Component | Orientation (north of east) | Amplitude (microstrain) |
|---|---|---|---|
| DonnaLee | DLT1 | 18.6 | –60 |
| | DLT2 | 78.6 | 150 |
| | DLT3 | –41.4 | –200 |
| Froelich | FLT1 | 50.2 | 1 |
| | FLT2 | –69.7 | –13 |
| | FLT3 | –9.7 | –4 |

TABLE 3. PRINCIPAL STRAINS IN THE LITHOSPHERE AS COMPUTED FROM TABLE 2

| | | $\varphi_0$ (°) | $e(\varphi_0)$ (μstrain) |
|---|---|---|---|
| DonnaLee (DLT) | Contraction: | 66.95 | 166.8 |
| | Extension: | –23.05 | –240.0 |
| Froelich (FLT) | Contraction: | 25.0 | 7.27 |
| | Extension: | –65.0 | –27.44 |

The results are shown in Figure 6 (not to scale). Notice that the strains are inverted as compared with the sign of the stresses in the lithosphere. The reason was explained above. We conclude that the principal extensional tectonic stresses fall within 20° of the trace of the San Andreas fault. At Froelich, the principal extension is nearly parallel to the observed GPS displacement vectors (Parsons, 2006). The principal contractions are almost normal to the fault trace. In the following calculation of the stresses, we use data from Froelich in preference over DonnaLee because of the relatively lesser variability of granite as compared to sandstone.

We may obtain an order-of-magnitude estimate of tectonic stresses from the creep term in Equation 7, which we may rewrite as follows:

$$\varepsilon(t_2) - \varepsilon(t_1) = \frac{\sigma_0 q}{M}\left[\log(1+\omega_0 t_2) - \log(1+\omega_0 t_1)\right], \tag{11}$$

where $1 + \omega_0 t \approx \omega_0 t$ is used as an approximation, since $\omega_0 t \gg 1$ (Lomnitz, 1957).

The principal tectonic stress $\sigma_0$ may be estimated from this expression as follows. From the long-term creep strain amplitudes at Froelich (Table 2), we find $\varepsilon(18.5) - \varepsilon(1.5) = 27.44$ μstrain in the principal extensional stress direction, for a time interval of $t = 18.5 - 1.5$ a. Assuming $\varepsilon(1.5) = 0$, we find, from Equation 11,

$$\frac{\sigma_0 q}{M} \approx \frac{27.44}{\log 18.5 - \log 1.5} = 10.97. \tag{12}$$

From the literature we assume a Young's modulus of $M = 50$ GPa (e.g., Webb, 1992), and a creep modulus $q = 0.01$ for granite. These values inserted in Equation 12 lead to a principal extensional tectonic stress of $\sigma_0 = 54.6$ MPa, or roughly 550 bars in the direction $\varphi_0 = -65°$, or 25° west of north. This rough estimate is not meant to substitute for a tectonic stress estimation based on experimental moduli recovered from rock cores and tested in the laboratory.

## DISCUSSION

### Tectonic Stress Estimation

Our tentative result of $\sigma_0 = 54.6$ MPa, or roughly 550 bars in the direction = –65°, or 25° west of north, is reasonably close to available measurements of tectonic stresses in the region (Townend and Zoback, 2004; Hickman and Zoback, 2004; Zoback and Zoback, 2002). Notice, however, that the ratios of contraction to extension at Froelich are quite different from those at DonnaLee (see Fig. 8). This suggests that the tectonic stress tensors may differ significantly on either side of the fault.

We did not attempt to use any strain data in the nanostrain range. Grout expansion during the initial 18 months of the experiment was not

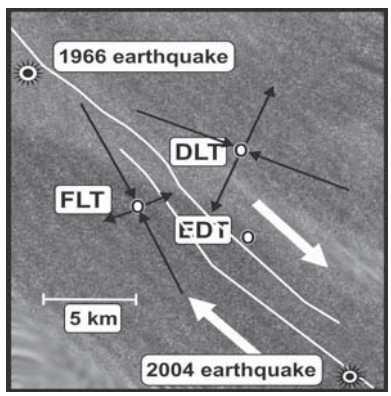


**Figure 8. Cumulative principal strains in the upper lithosphere at Parkfield as estimated from the 1987–2004 long-term creep components at stations Froelich (FLT) and DonnaLee (DLT) (not to scale). White lines—main traces of the San Andreas fault. Black arrows—principal strains. Amplitudes at FLT are magnified by a factor of 10 as compared to DLT.**

taken into account because no experimental data on the long-term stress-strain behavior of the grout was available. All strains were referred to the zero crossing at $t$ = 1.5 a: thus the useful time interval for strain calculations was reduced to 16.5 years, even though 18 years of strain data were available. In the absence of cores, this is probably the best we can do.

### Extinctions in the Response Curve of Strainmeters

The theory of the strainmeter was developed in three-quarters of a century after Benioff (1935) invented his quartz-cantilever strainmeter. A flat frequency response in the range of long wavelengths is still frequently assumed.

If a seismic wavefront hits the strainmeter broadside, the two ends of the instrument are in phase and the response is null for all wavelengths. Even in the case of oblique incidence (up to $\cos\phi = L/l$, where $L$ = 12.5 cm and $l$ is the wavelength), the instrument has an infinity of extinctions or blind spots in the *f-k* domain corresponding to $\lambda = L/n$, $n$ = 1, 2, . . ., where the apparent wavelength

$$\lambda = l\cos\phi \tag{13}$$

is the projection of the incident wavelength $l$ onto the direction of the strainmeter (Lomnitz, 1997).

Because the azimuth $\phi$ is independent of the wavelength, the apparent wavelength $\lambda$ could be less than $L$ even for long waves. The response function $R = \varepsilon^*/\varepsilon$ is the ratio between the observed strain $\varepsilon^*$ and the true earth strain $\varepsilon$

$$R = \frac{\sin\xi}{\xi}, \text{ where } \xi = \pi L/\lambda, \tag{14}$$

which defines two distinct domains: *high-frequency response* ($\lambda < L$) and *low-frequency response* ($\lambda > L$). The high-frequency domain is normally confined to a narrow azimuth range such that $|\cos\phi| < L/l$, but it can contain blind spots and regions of phase reversal where $R < 0$. These distortions can be troublesome. A propagating stress step $\sigma_0 H(0)$ contains sine waves of all frequencies because of the Heaviside function $H(0)$. As noticed by Agnew and Gomberg (1996), even laser strainmeters may significantly underestimate the amplitude of stress drops from earthquakes as compared to seismic measurements, because high-frequency waves close to a blind spot are eliminated.

Another potentially serious distortion is due to presence of inverted response, $R < 0$, in the high-frequency domain (Fig. 9). Using strainmeters for first-motion studies is not recommended because of this problem.

### Strain versus GPS

Geodetic measurements are widely used to infer the tectonic strains that may accumulate before earthquakes. The measurements are converted first to relative displacements, and then to strains by comparing relative positions of two or more GPS stations, using a set of assumptions. The main issue is how to convert relative displacements to strains in the presence of large creep deformations (Burford, 1988). The practice of GPS data reduction in California is aptly summarized by Parsons (2006), including a discussion on the use of power-law creep:

$$\dot{\varepsilon}_c = A\sigma_d^n \exp\left(-\frac{Q}{RT}\right), \tag{15}$$

where $\dot{\varepsilon}_C$ is the effective steady-state creep rate, $A$ is the creep coefficient in $MPa^{-n}s^{-1}$, $\sigma_d = \sigma_1 - \sigma_3$ is the effective or deviatoric stress in MPa, $n$ is the creep exponent (usually taken to be 3.0–3.5), $Q$ is the activation energy in J/mol, $R$ is the universal gas constant, and $T$ is the temperature (e.g., Albert and Phillips, 2002). Equation 15 is appropriate for conditions in the plastic upper mantle, where temperatures are high and steady-state creep is significant. It lacks experimental support in the lithosphere.

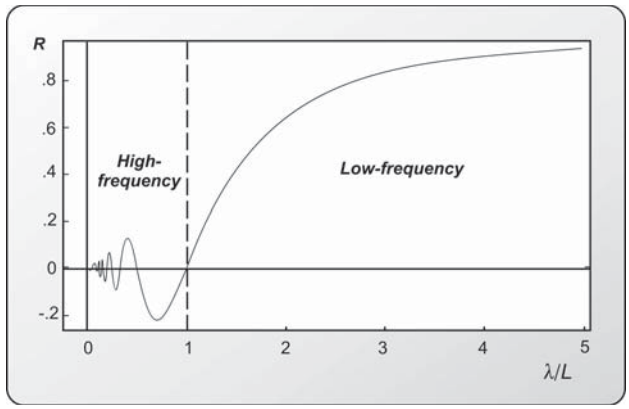


**Figure 9. Response of a strainmeter of base length *L* to an incident seismic wave of apparent wavelength λ (after Lomnitz, 1997). The frequency domains are separated by the dotted line.**

The values of $A$ and $T$ in the seismogenic zone are very low. As a result, estimates for $\dot{\varepsilon}_C$ tend to vanish. GPS displacements are attributed entirely to the accumulation of elastic energy as creep rates are held to be negligible (Parsons, 2006). However, creep rates in the lithosphere are actually quite significant. Even after 18 years of observations the creep rates at Parkfield were on the order of microstrains/year. Continuous creep rates on the San Andreas system have been observed for many years (e.g., Savage and Lisowski, 1993). In the case of the segment north of Parkfield creep accounts for a significant share of the relative plate velocities. In conclusion, Equation 15 might not be applicable to the cool lithosphere.

## CONCLUSIONS

We explore the long-term borehole strainmeter records provided by the Parkfield experiment (1985–2004) in search of a new interpretation. The attempt proves rewarding, because long-term creep observations in the lithosphere are rare. We find that the theory of strainmeters contains notorious gaps, as does that of boreholes.

(1) The stress-strain-time relation in the upper lithosphere is accurately represented by a Volterra equation:

$$\varepsilon(t) = \frac{1}{M}\left[\sigma(t) + \int_0^\infty \sigma(\tau)\varphi(t-\tau)d\tau\right],$$

where the decay function $\varphi(t)$ is found to be

$$\varphi(t) = \frac{q\omega_0}{1+\omega_0 t}.$$

This form of the constitutive equation can be derived from considerations of ergodicity.

(2) A theory of cavities in a halfspace is outlined. Noether's theorem ("every symmetry in a system leads to a physically conserved quantity") affords a new understanding of why the stress energy field is conserved in conformal transformations. We demonstrate another use of conformal mapping to procure an understanding of borehole technology. A cavity reverses the sign of the strains generated at the boundary in a stress field.

(3) A borehole strainmeter in a ring of expansive grout is deformed into an ellipse, such that the major axis is orthogonal to the elliptical deformation of the borehole. Zero crossings occur when the expansive energy of the grout is exhausted.

(4) Long-term strain records over the 1986–2004 interseismic interval provide no evidence of strain accumulation prior to the 2004 earthquake. The state of stress in the lithosphere may have remained stationary at ~55 MPa during the 19 years that preceded the earthquake.

Is earthquake prediction now to be shelved as "unsuccessful" or "still not achievable" (Jackson and Kagan, 2006; Bakun et al., 2005)? Should we try harder?

A theory is worthless if it cannot predict. Parkfield observations are less than encouraging: they constrain nucleation of the 2004 earthquake to a tiny source region with a diameter of less than 30 m (Johnston et al., 2006). Thus an earthquake of magnitude 6 might be triggered by an event of magnitude 2.2, but events of this size occur on the San Andreas fault at an estimated mean rate of 3.1 per day. A significant strain perturbation might even be caused by drilling a strainmeter borehole into the fault, but no convincing cases of triggering of earthquakes by boreholes have been found. More likely, the argument that large earthquakes can be triggered by smaller ones is a non sequitur of the type "The conductor's whistle triggers the departure of the train."

The 1985–2004 Parkfield experiment is well worth another visit.

## ACKNOWLEDGMENTS

We are indebted to Diego Melgar, Alan Linde, Sergio Chávez, Ross Gwyther, Peter Malischewsky, Ralph Lorenz, Roland Bürgmann, Malcolm R. Forster, Andrew Michael, Pablo Padilla, James Savage, Walter Zuern, and two anonymous reviewers, for valuable criticism and suggestions.

## REFERENCES CITED

Agnew, D., and Gomberg, J., 1996, The accuracy of seismic estimates of dynamic strains: An evaluation using strainmeter and seismometer data from Piñon Flat observatory, California: Bulletin of the Seismological Society of America, v. 86, p. 212–220.

Albert, R.A., and Phillips, R.J., 2002, Time-dependent effects in elastoviscoplastic models of loaded lithosphere: Geophysical Journal International, v. 151, p. 612–621, doi: 10.1046/j.1365-246X.2002.01803.x.

Arnold, V.I., and Avez, A., 1968, Ergodic Problems of Classical Mechanics: New York, W.A. Benjamin, 286 p.

Baez, J., 2002, Noether's theorem in a nutshell, http://math.ucr.edu/home/baez/noether.html.

Bakun, W.H., Aagaard, B., Dost, B., Ellsworth, W.L., Hardebeck, J.L., Harris, R.A., Ji, C., Johnston, M.J.S., Langbein, J., Lienkaemper, J.J., Michael, A.J., Murray, J.R., Nadeau, R.M., Reasenberg, P.A., Reichle, M.S., Roeloffs, E.A., Shakal, A., Simpson, R.W., and Waldhauser, F., 2005, Implications for prediction and hazard assessment from the 2004 Parkfield earthquake: Nature, v. 437, p. 969–974, doi: 10.1038/nature04067.

Bath, M., and Berkhout, A.J., 1984, Mathematical Aspects of Seismology: London, Geophysical Press, Handbook of Geophysical Exploration, v. 17, p. 33–42.

Benioff, H., 1935, A linear strain seismograph: Bulletin of the Seismological Society of America, v. 25, p. 283–309.

Blanpied, M.L., Marone, C.J., Lockner, D.A., Byerlee, J.D., and King, D.P., 1998, Quantitative measure of the variation in fault rheology due to fluid-rock interactions: Journal of Geophysical Research, v. 103, no. B5, p. 9691–9712, doi: 10.1029/98JB00162.

Burford, R.O., 1988, Retardations in fault creep rates before local moderate earthquakes along the San Andreas fault system, central California: Pure and Applied Geophysics, v. 126, p. 499–529, doi: 10.1007/BF00879008.

Claerbout, J., and Dellinger, J., 1987, Eisner's reciprocity paradox and its resolution: Tulsa, Oklahoma, Leading Edge, v. 6, p. 34–37, doi: 10.1190/1.1439337.

Cleland, A.N., 2003, Foundations of Nanomechanics: From Solid-State Theory to Device Applications: New York, Springer, Section 9.7, p. 340–348.

Enescu, B., Mori, J., Miyazawa, M., and Kano, Y., 2009, Omori-Utsu law c-values associated with recent moderate earthquakes in Japan: Bulletin of the Seismological Society of America, v. 99, p. 884–891, doi: 10.1785/0120080211.

Gladwin, M.T., and Hart, R., 1985, Design parameters for borehole strain instrumentation: Pure and Applied Geophysics, v. 123, p. 59–80, doi: 10.1007/BF00877049.

Griggs, D.T., and Handin, J., eds., 1960, Rock deformation: A symposium: Geological Society of America Memoir 79, 382 p.

Gwyther, R., 1995, An investigation of aseismic fault processes in California with borehole strain measurements [Ph.D. thesis]: Australia, University of Queensland, 188 p.

Harris, R.A., and Arrowsmith, J.A., 2006, Introduction to the special issue on the 2004 Parkfield earthquake and the Parkfield earthquake prediction experiment: Bulletin of the Seismological Society of America, v. 96, p. S1–S10, doi: 10.1785/0120050831.

Hart, R.H.G., Gladwin, M.T., Gwyther, R.L., Agnew, D.C., and Wyatt, F.K., 1996, Tidal calibration of borehole strain meters: Removing the effects of small-scale inhomogeneity: Journal of Geophysical Research, v. 101, no. B11, p. 25,553–25,571, doi: 10.1029/96JB02273.

Hickman, S., and Zoback, M., 2004, Stress orientations and magnitudes in the SAFOD pilot hole: Geophysical Research Letters, v. 31, doi: 10.1029/2004GL020043.

Jackson, D.D., and Kagan, Y.Y., 2006, The 2004 Parkfield earthquake, the 1985 prediction, and characteristic earthquakes: Lessons for the future: Bulletin of the Seismological Society of America, v. 96, p. S397–S409, doi: 10.1785/0120050821.

Jeffreys, H., 1970, The Earth (fifth edition): Cambridge, UK, Cambridge University Press, 525 p.

Jeong, H.-s., Kang, S.-s., and Obara, Y., 2007, Influence of surrounding environments and strain rates on the strength of rocks subjected to uniaxial compression: International Journal of Rock Mechanics and Mining Sciences, v. 44, p. 321–331, doi: 10.1016/j.ijrmms.2006.07.009.

Johnston, M.S.J., Borcherdt, R.D., Linde, A.T., and Gladwin, M.T., 2006, Continuous borehole strain and pore pressure in the near field of the 28 September 2004 M 6.0 Parkfield, California, earthquake: Implications for nucleation, fault response, earthquake prediction, and tremor: Bulletin of the Seismological Society of America, v. 96, p. S56–S72, doi: 10.1785/0120050822.

Kirsch, G., 1898, Die Theorie der Elastizität und die Bedürfnisse der Festigkeitslehre: Zeitschr. Vereinig. Deutscher Ingenieure, v. 42, p. 797–807.

Langbein, J., Murray, J.R., and Snyder, H.A., 2006, Coseismic and initial postseismic deformation from the 2004 Parkfield, California, earthquake, observed by global positioning system, electronic distance meter, creepmeters, and borehole strainmeters: Bulletin of the Seismological Society of America, v. 96, p. S304–S320, doi: 10.1785/0120050823.

Li, Y.-G., Chen, P., Cochran, E.S., Vidale, J.E., and Burdette, T., 2006, Seismic evidence for rock damage and healing on the San Andreas fault associated with the 2004 M 6.0 Parkfield earthquake: Bulletin of the Seismological Society of America, v. 96, p. S349–S363, doi: 10.1785/0120050803.

Lockner, D.A., 1995, Rock failure, *in* Ahrens, T.J., ed., Rock Physics and Phase Relations: American Geophysical Union, 236 p.

Lomnitz, C., 1956, Creep measurements in igneous rocks: The Journal of Geology, v. 64, p. 473–479.

Lomnitz, C., 1957, Linear dissipation in solids: Journal of Applied Physics, v. 28, p. 201–205, doi: 10.1063/1.1722707.

Lomnitz, C., 1997, Frequency response of a strainmeter: Bulletin of the Seismological Society of America, v. 87, p. 1078–1080.

Lund, B., 2000, Crustal stress studies using microearthquakes and boreholes [Ph.D. thesis]: Uppsala University, Department of Earth Sciences, 75 p., http://www.geofys.uu.se/bl/Avh/index.html.

Marinho, R.M., Jr., 2007, Noether's theorem in classical mechanics revisited: European Journal of Physics, v. 28, p. 37–43, doi: 10.1088/0143-0807/28/1/004.

Murray, J., and Langbein, J., 2006, Slip on the San Andreas fault at Parkfield, California, over two earthquake cycles, and the implications for seismic hazard: Bulletin of the Seismological Society of America, v. 96, p. S283–S303, doi: 10.1785/0120050820.

NIRE, 1998, Stress corrosion cracking of rock in chemical environment: Tokyo, National Institute of Advanced Industrial Science and Technology (AIST), Annual Report (English summary), p. 29.

Parsons, T., 2006, Tectonic stressing in California modeled from GPS observations: Journal of Geophysical Research, v. 111, B03407, doi: 10.1029/2005JB003946.

Potyondy, D.O., 2007, Simulating stress corrosion with a bonded-particle model for rock: International Journal of Rock Mechanics and Mining Sciences, v. 44, p. 677–691, doi: 10.1016/j.ijrmms.2006.10.002.

Roeloffs, E., 2005, Long-term trends in borehole strainmeter and tiltmeter data: Menlo Park, California, U.S. Geological Survey, Class notes for UNAVCO, 10 p., http://www.unavco.org:8080/cws/straindata/Notesfrom2005class/detrend_long-term.pdf.

Roeloffs, E., Hodgkinson, K., and Bryan, C., 2004, Review of borehole strainmeter data collected by the U.S. Geological Survey, 1985–2004: U.S. Geological Survey Report, May 25, 2004 (draft version).

Savage, J.C., and Lisowski, M., 1993, Inferred depth of creep on the Hayward fault, central California: Journal of Geophysical Research, v. 98, p. 787–793, doi: 10.1029/92JB01871.

Singh, T.N., and Verma, A.K., 2005, Prediction of creep characteristic of rock under varying environment: Environmental Geology, v. 48, p. 559–568, doi: 10.1007/s00254-005-1312-4.

Szczepanik, Z., Milne, D., Kostakis, K., and Eberhardt, E., 2003, Long term laboratory strength tests in hard rock, *in* Handley, M., and Stacey, D., eds., Technology roadmap for rock mechanics: Pretoria, South African Institute of Mining and Metallurgy, Tenth Congress of the International Society for Rock Mechanics, Johannesburg, p. 1179–1184.

Townend, J., and Zoback, M.D., 2004, Regional tectonic stress near the San Andreas fault in central and southern California: Geophysical Research Letters, v. 31, L15S11, doi: 10.1029/2003GL018918.

Webb, S.L., 1992, Low-frequency shear and structural relaxation in rhyolite melt: Physics and Chemistry of Minerals, v. 19, p. 240–245, doi: 10.1007/BF00202314.

Zoback, M.D., and Zoback, M.L., 2002, State of stress in the Earth's lithosphere, *in* Lee, W.H.K., Kanamori, H., Jennings, P.C., and Kisslinger, C., eds., International Handbook of Earthquake and Engineering Seismology, Part A: New York, Academic Press, p. 559–568.

MANUSCRIPT RECEIVED 13 AUGUST 2008
REVISED MANUSCRIPT RECEIVED 30 APRIL 2009
MANUSCRIPT ACCEPTED 4 MAY 2009

Printed in the USA